Möbius Metamaterial Inspired Next Generation Electronic Circuits and Systems

Authors:

Ajay K. Poddar (1) , Ulrich L. Rohde (1, 2,),

Author affiliations:

(1) Synergy Microwave, NJ, USA

(2) Massachusetts Institute of Technology, MIT, Microsystems Technology Laboratories, USA

Based on [1,2,3]

From metallic alloys to plastic composites, scientists and engineers have been developing artificial materials for various applications. Metamaterial is a family of artificial composite structure made from conventional material with an unconventional structure, exhibits distinct properties such as negative index characteristics for selective frequency regions what nature can provide easily[1-8]. Their shape, size, geometry, orientation, and arrangement gives them their smart properties, capable of manipulating EM (electromagnetic) waves by bending, blocking, absorbing, and enhancing to attain benefits that go beyond what is possible with conventional materials. Metamaterial structures that show Möbius symmetry where coupling strengths and size of the structure scales can be engineered, are a promising candidate of topology driven Mobius coupled structures for next generation electronics in which lower profile and energy saving electronics are desired by users[2]. Distinctive contributions in the field of MMI (Möbius Metamaterial Inspired) technology allow topological exploration, yielding high Q factor, based on evanescent mode resonance[3]. The reported multi-knots MMS (Möbius-Metamaterial-Strips) structure enables multi-injection-nodes for multi-phase-injection-locking, facilitating concurrent signal-source solutions[4]. MMI based technology enables energy harvesting approach for the realization of next generation energy-saving electronics such as spintronic devices, quantum oscillator, RFID (Radio-Frequency-Identification-Device), Signal Retention Device, proximity-sensors, enhanced dynamic range for underground detection, detection of trapped victim heartbeat, and biosensors applications[5-6].

What makes MMI structure unique is topology and size, for example, MMI structure interacts with forces at the Nanoscale, the interface dynamics can be explained by quantum mechanics. The same structure scaled to much larger than its wavelength, would no longer exhibit the same properties. The characteristics of the structure can be described by conventional structural engineering and material science. The application of MMI structure at Nanoscale can exhibit repulsive Casimir force[9-11], which has important practical applications in creating anti-gravity and Levitations[12]. Figure (1) shows the practical evidence of Casimir force 'F' on parallel plates kept in vacuum, the effective force $F \propto A/d^4$, where A is the area of plate and d is the distance between the plates.

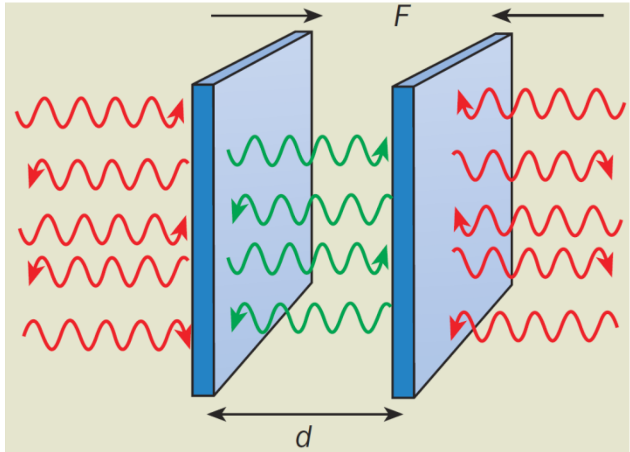

Fig.1: Shows the practical evidence of Casimir force 'F' on parallel plate kept in vacuum, the effective force F $\propto A/d^4$, where A is the area of plate and d is the distance between the plate [9].

Figure (2) shows the repulsive Casimir force '*F*' on parallel plate kept in vacuum, the effective force $F \propto -A/d^4$, where *A* is the area of plate and *d* is the distance between the plate. Figure (3) shows the typical example of levitating mirror (The repulsive Casimir force of a metamaterial may balance the weight of one of the mirrors, letting it levitate on zero-point fluctuation).

The Casimir force[9] (Figure 1) arises from the interaction of the surfaces with the surrounding electromagnetic spectrum, and includes a complex dependence on the full dielectric function of both surfaces and the region between. The complexity of the Casimir force leads to significantly greater possibility for manipulation through materials, geometries, and other phenomena. The significantly greater complexity of the Casimir force potentially allows greater opportunity for neutralization or for use of Casimir forces to partially cancel Van Der Waals forces. On the more theoretical side, MMI structure can produce a powerful Casimir Effect (Force from nothing), which will allow us to transport the matter; this implies that we can use this effect to attract or push away physical matter. Some of the practical applications include building auto focusing camera lens, more efficient servos, silicon array propulsion systems and high speed rail systems. The implications of a repulsive Casimir force for the MEMS (Micro-Electromechanical System) industry could be significant with potential applications including stiction prevention in sensors, contactless bearings and contactless power transmission[10]. MEMS (Micro-Electromechanical system) based electronics offer inexpensive high performance solutions. But reliability issues arising from stiction in MEMS switching devices, prevents the technology for high frequency applications.

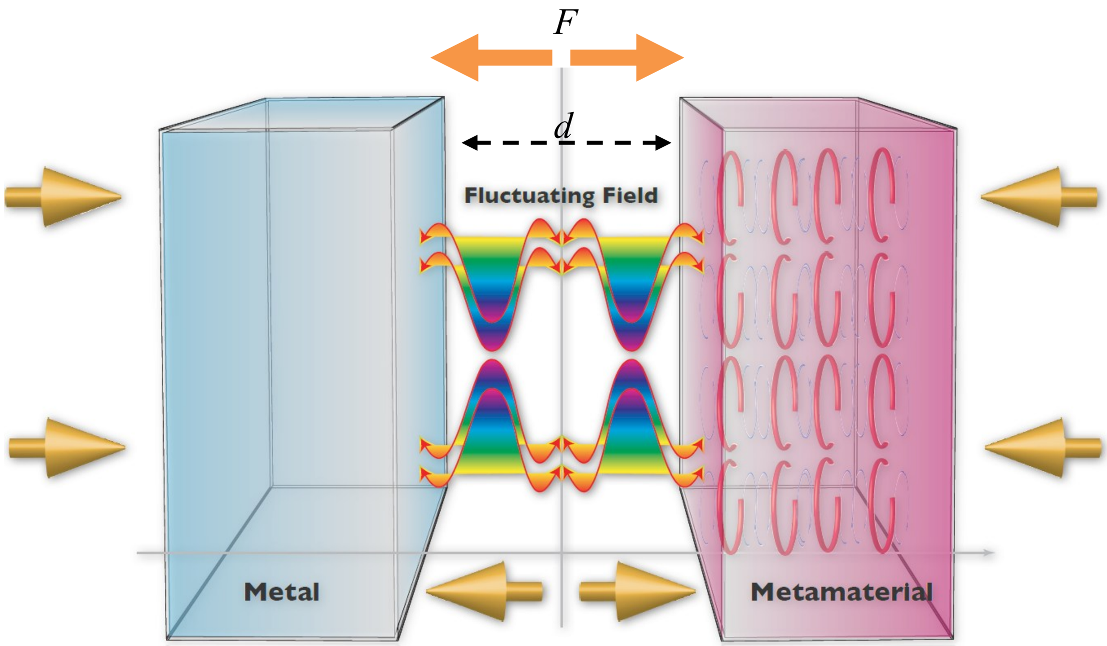

Fig.2: Shows the repulsive Casimir force 'F' on parallel plate kept in vacuum, the effective force F $\propto$- A/d^4, where A is the area of plate and d is the distance between the plate [11].

The pioneering contributions relate to techniques for stiction-free MEMS lateral switch and its application in switching network, phase shifters in electronically scanned phase array antennas for Internet of Things (IoT) applications. In vacuum, the force of attraction between two surfaces in nanometer range is explained by Casimir Effect, but effective repulsive forces can be noticed when the two surfaces with materials of different permittivity are taken into consideration[11-12]. This phenomenon can also be observed if one of the surfaces possesses negative permittivity. This approach can resolve the stickiness problem, leading to new material and fabrication methods in next generation electromechanics.

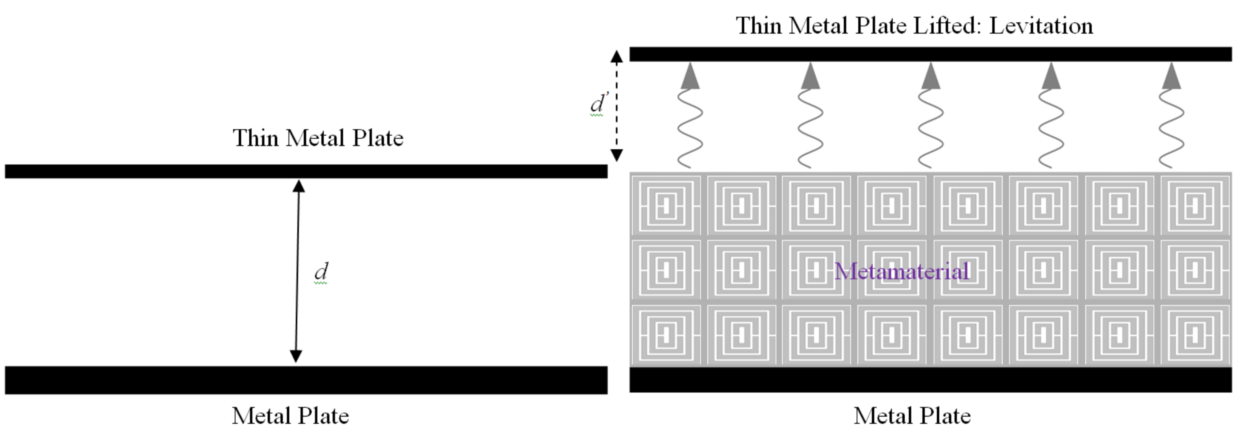

Fig. 3: Levitating mirror (The repulsive Casimir force of a metamaterial may balance the weight of one of the mirrors, letting it levitate on zero-point fluctuation) [12].

One of the exciting properties of MMI structure is that they can bend light in a way that is mathematically equivalent to the way space-time bends light, allows topological exploration for the realization of low cost gravitational wave detector. Figure (4) shows the Gravitational Casimir effect, with a two plate setup, the change in the refractive index of the plates causes the gravitational wave to refract, where k represents the wave vector of the incident, transmitted, and reflected gravitational waves, and γ is the corresponding angle with respect to the surface normal [13].

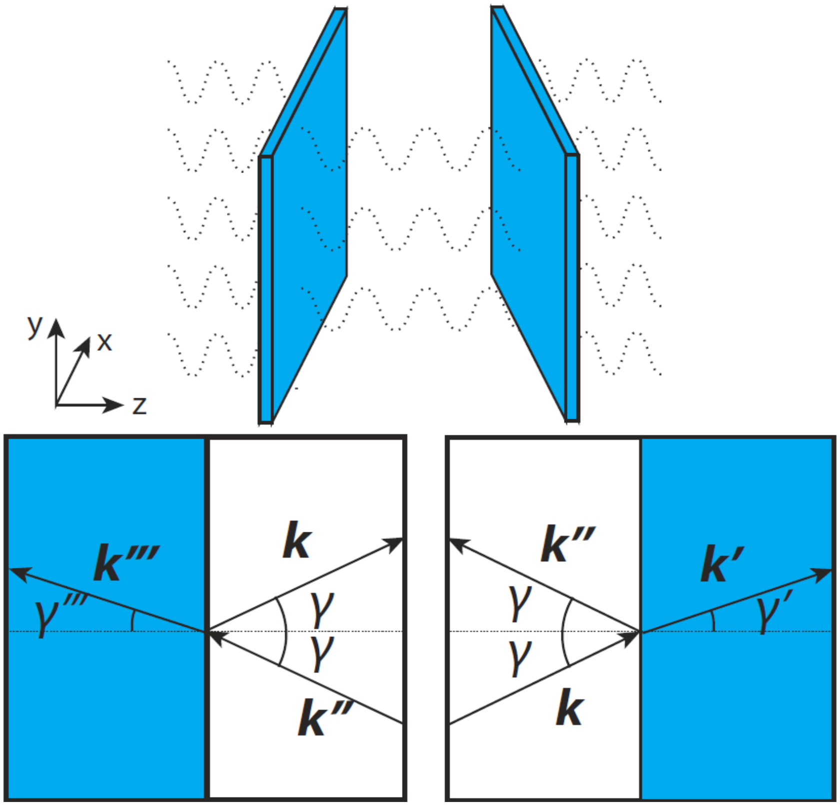

Fig. 4: Shows the Gravitational Casimir effect, with a two plate setup, the change in the refractive index of the plates causes the gravitational wave to refract, where k represents the wave vector of the incident, transmitted, and reflected gravitational waves, and γ is the corresponding angle with respect to the surface normal [13].

The details of Casimir Effect and applications using MMI (Möbius Metamaterial Inspired) structure for futuristic applications will be discussed in Part-2 (June 2016 Issue) and Part-3 (July 2016 Issue.

The current issue (Part-1) briefly describes the applications of MMI structure for Internet of Things (IoT), CubeSat, and Examples of Möbius transformation and Metamaterial symmetry for Medical Telemetry, Imaging, and Sensors applications.

(A) Internet of Things (IoT)

The Internet of Things (IoT) is the network of physical objects: devices, vehicles, buildings and other items embedded with electronics, software, sensors, and network connectivity that enable these objects to collect and exchange data. Figure (5) shows the symbolic sketch of the IoT (Internet of Things), connects devices and vehicles using electronic sensors and the Internet for next generation communication networks[14]. The IoT allows objects to be sensed and controlled remotely across existing network infrastructure, creating opportunities for more direct integration of the physical world into computer-based systems, and resulting in improved efficiency, accuracy and economic benefit; when IoT is augmented with sensors and actuators, the technology becomes an instance of the more general class of cyber-physical systems, which also encompasses technologies such as smart grids, smart homes, intelligent transportation and smart cities. Each thing is uniquely identifiable through its embedded computing system but is able to interoperate within the existing Internet infrastructure.

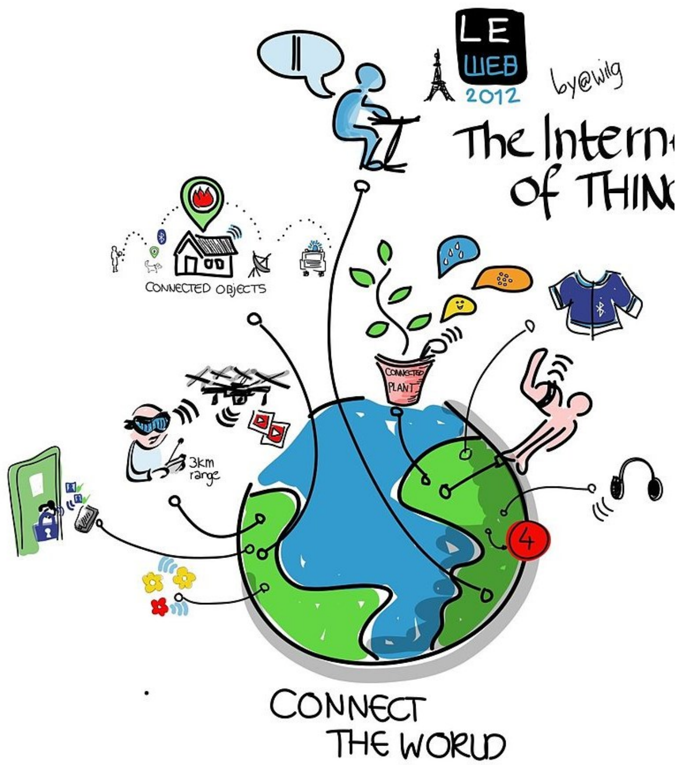

Fig. 5: Shows the symbolic sketch of the IoT (Internet of Things), connects devices and vehicles using electronic sensors and the Internet for next generation communication networks [14].

Figure (6) illustrates the Technology Roadmap of Internet of Things [14]. As depicted in Figure (6), current technology cannot meet the challenges posed by faster, reliable and ubiquitous radio systems for the requirement of IoT. The trend over past decades has been to place an ever increasing emphasis on digital signal processing (DSP), where spectral efficiency has been maximized via sophisticated modulation, multiplexing or MIMO schemes. However, these approaches have now reached their limits and migration to millimeter wave and terahertz frequencies has become indispensable to access larger spectral resources. Unfortunately, DSP is not applicable at such frequencies, where signals are varying too fast to be digitized. The unprecedented control of electromagnetic properties afforded by MMI (Möbius Metamaterial Inspired) structure open the door to provide faster processing and low power miniaturized electronics to overcome the technological challenges faced by engineers.

Recent publication describes the real-time analog signal processing(R-ASP) of electromagnetic wave at very high frequencies in real time using metamaterial inspired technology in conjunction with concepts of ultrafast optics [15-17]. There a need of a special branch of Metamaterial engineering discussing manipulation of EM-wave in Space, Time and Space-Time for the realization of unlimited number of distinct types of artificial smart materials (Electromagnetic Band gap Metamaterial, Single Negative Metamaterial, Double Negative Metamaterial, Bi-Isotropic And Bi-Anisotropic Metamaterial, Chiral Metamaterial), suited for applications in following:

(a) Telecommunication

(b) Medical Instrumentation

- *Bio-Medical*
- *Oral & Oncology*

- *Ultrasound Imaging*
- *Magnetic Resonance Imaging*

(c) Optics

(d) Sensing

- *Bio Sensor*
- *Thin film sensor*
- *Wireless Strain Sensor*
- *Aerospace & Defense*

(e) Energy Harvesting

(f) Transportation of Matter

(g) Casimir Effect (Attractive and Repulsive Forces)

- *Levitations and Anti-Gravity*

The above listed applications can support the technology roadmap of IoT in reality illustrated in Figure (6)[14]. Figure (7) depicts the typical sketch of Metamaterial engineering, illustrating the solutions for next generation electronic circuits and systems[8].

As shown in Figure (7), $\bar{\bar{\chi}}(\omega, k;\, t, r)$ is the generic notation of tensors that represents the metamaterial permittivity ($\bar{\bar{\epsilon}}$), permeability ($\bar{\bar{\mu}}$), magnetic-to-electric coupling ($\bar{\bar{\xi}}$) and electric-to-magnetic coupling ($\bar{\bar{\zeta}}$) tensors, while ω is the angular frequency (reciprocal time), ***k*** is the spatial frequency (reciprocal space), ***t*** is time (direct time) and ***r*** is space (direct space). Combining different dependencies ($\omega, k; t, r$) and bianisotropies ($\bar{\bar{\epsilon}}, \bar{\bar{\mu}}, \bar{\bar{\xi}}, \bar{\bar{\zeta}}$) leads to a virtually unlimited number of distinct types of Metamaterials[8].

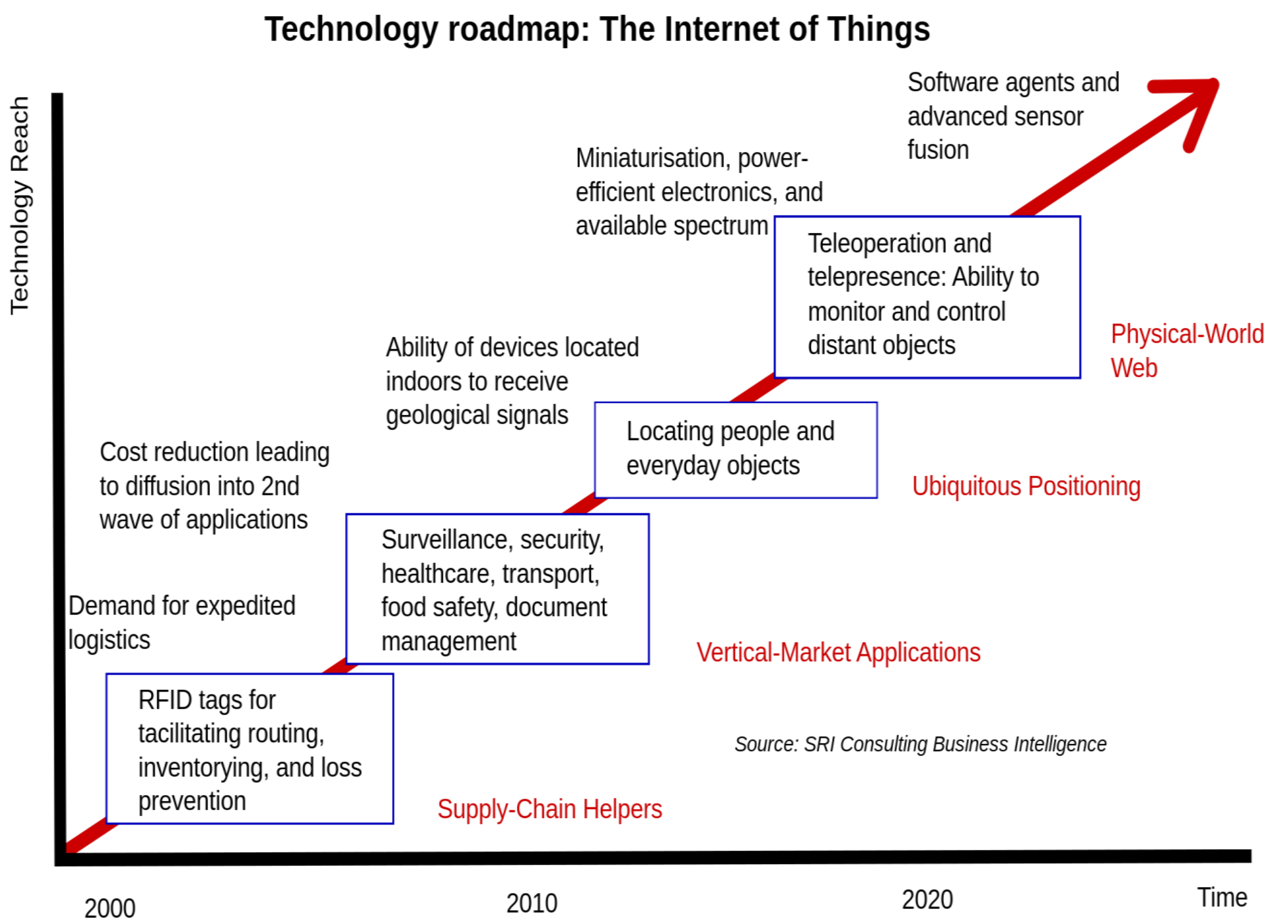

Fig. 6: Shows Technology Roadmap: Internet of Things [14]

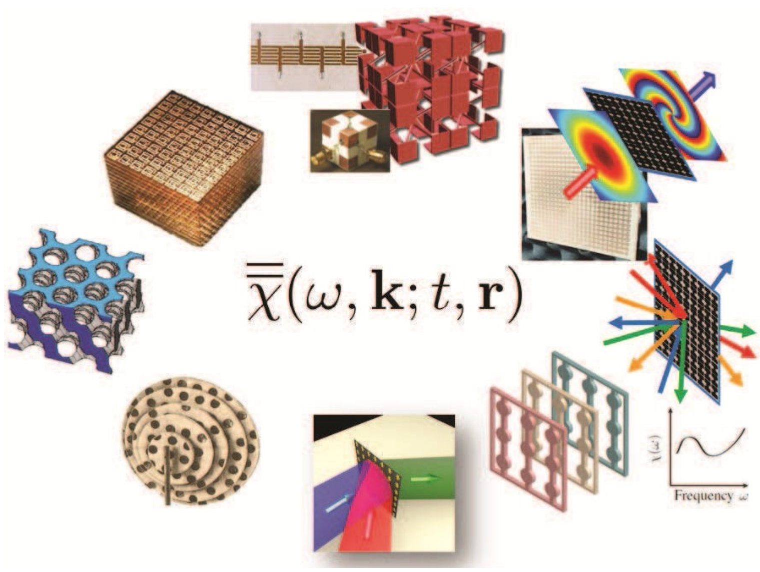

Fig.7: Shows the typical sketch of special branch of Metamaterial engineering, opens the door to diverse applications such as superlens, antennas, invisibility cloak, energy harvesters, and sensors [8].

(B) CubeSat

Satellites play a decisive role for establishing communication network; these satellites are expensive, large in size and take a number of years to build up. To keep the cost low, small satellites such as the CubeSat, have big reward over their larger counterparts. Small satellites are located in LEO (low-earth orbit) in the range of 200-2,000 km; the speed of small satellites in LEO (relative to Earth's surface) is around 7.5km/s, which is an orbital period of approximately 90 minutes. The definition of CubeSat comes from shape and weight of satellite, it belongs to the family of small satellite classification (Picosatellite <1kg, Nanosatellite 1-10kg, and Microsatellite 10-100kg). Figure (8) shows a typical CAD model of CubeSat (10cm × 10cm × 10cm) for giving brief insights about the compact layout[18]. Figure (9) shows the typical CubeSat bus structure for giving brief insights about the electronics inside the CubeSat hardware. Figure (10) depicts the actual CubeSat unit in hand and also its position in low-earth orbit [20].

Small satellites cost much less per unit, many CubeSat can be fabricated for the price of one Satellite. The pros of CubeSats are lower cost but cons are that the required hardware of a large satellite cannot fit in the small shoe box such as CubeSats. The possible cost-effective alternative is launching many CubeSats as depicted in Figure (11), and construct a network of small satellites that can accomplish the same tasks what one large satellite can. The advantage is if one of these CubeSat in the network someway fails, the network can be reconfigured to pick up the slack. But in the case of larger satellites, if something goes wrong, the entire mission is at risk of failure because of single fallout.

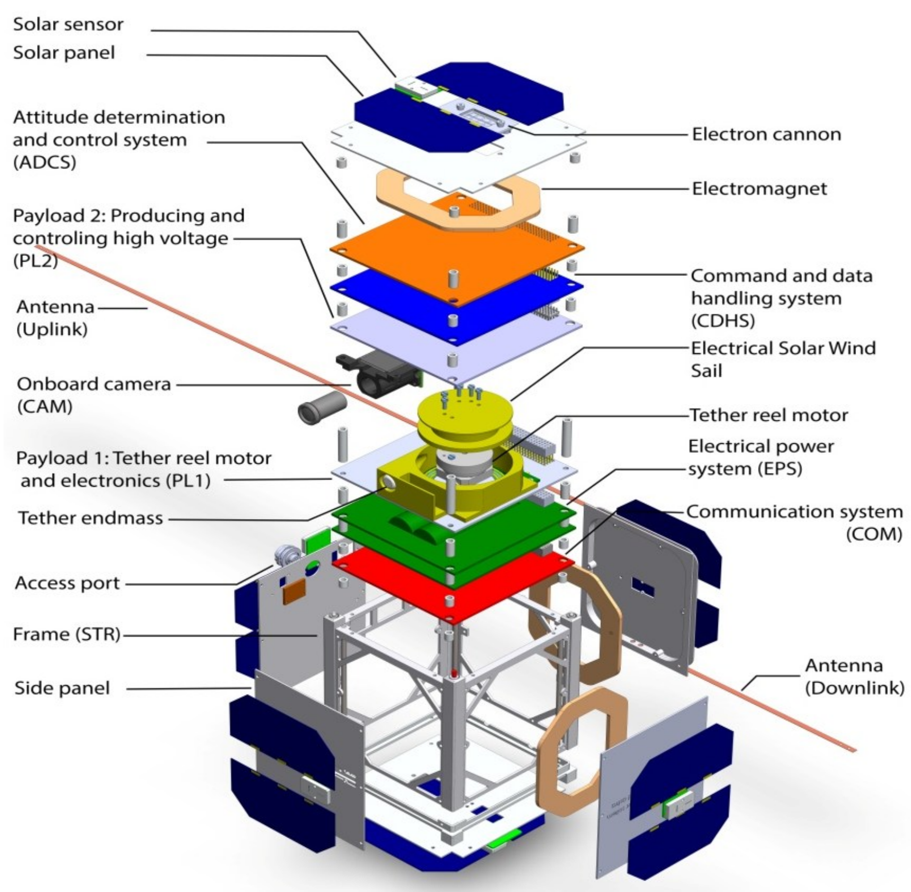

Figure 8: shows the view of the typical layout of CubeSat (Courtesy ESTCube-1) [18]

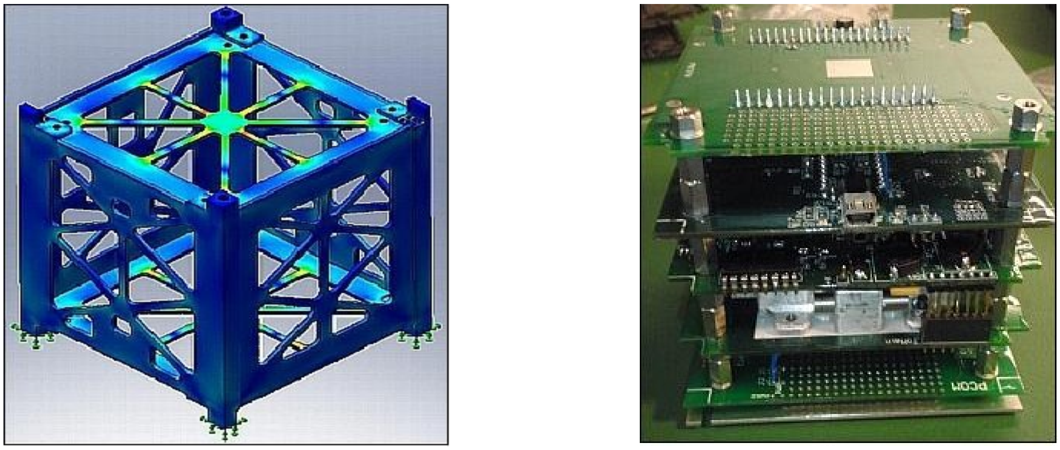

(a) Illustration of the CubeSat bus structure configuration

(b) Photo of the interior bus

Figure 9: shows the photograph of CubeSat (10cm × 10cm × 10cm), Courtesy: Colorado Space Grant Consortium, USA) [19]

(a) CubeSat hardware (10cm × 10cm × 10cm)

(b) CubeSat located in LEO (low-earth orbit)

Figure 10: shows the photograph of CubeSat (Courtesy: NASA) [20].

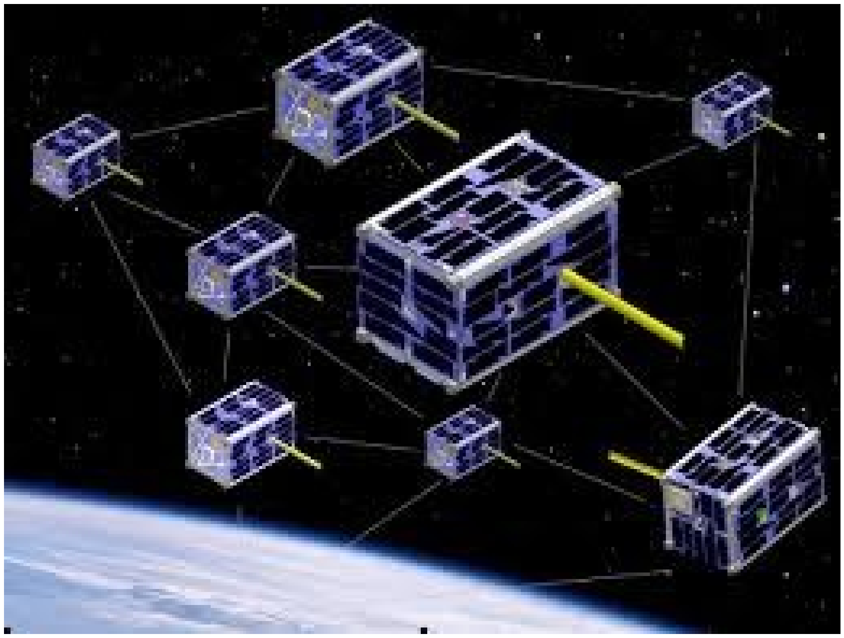

Figure 11: shows the network of multiple CubeSats (Courtesy NASA) [20]

Figure (12) illustrates the sketch view of the CubeSat launch[19-22]. Figure (13) shows the general block schematic structure of the designated personal communication[22].

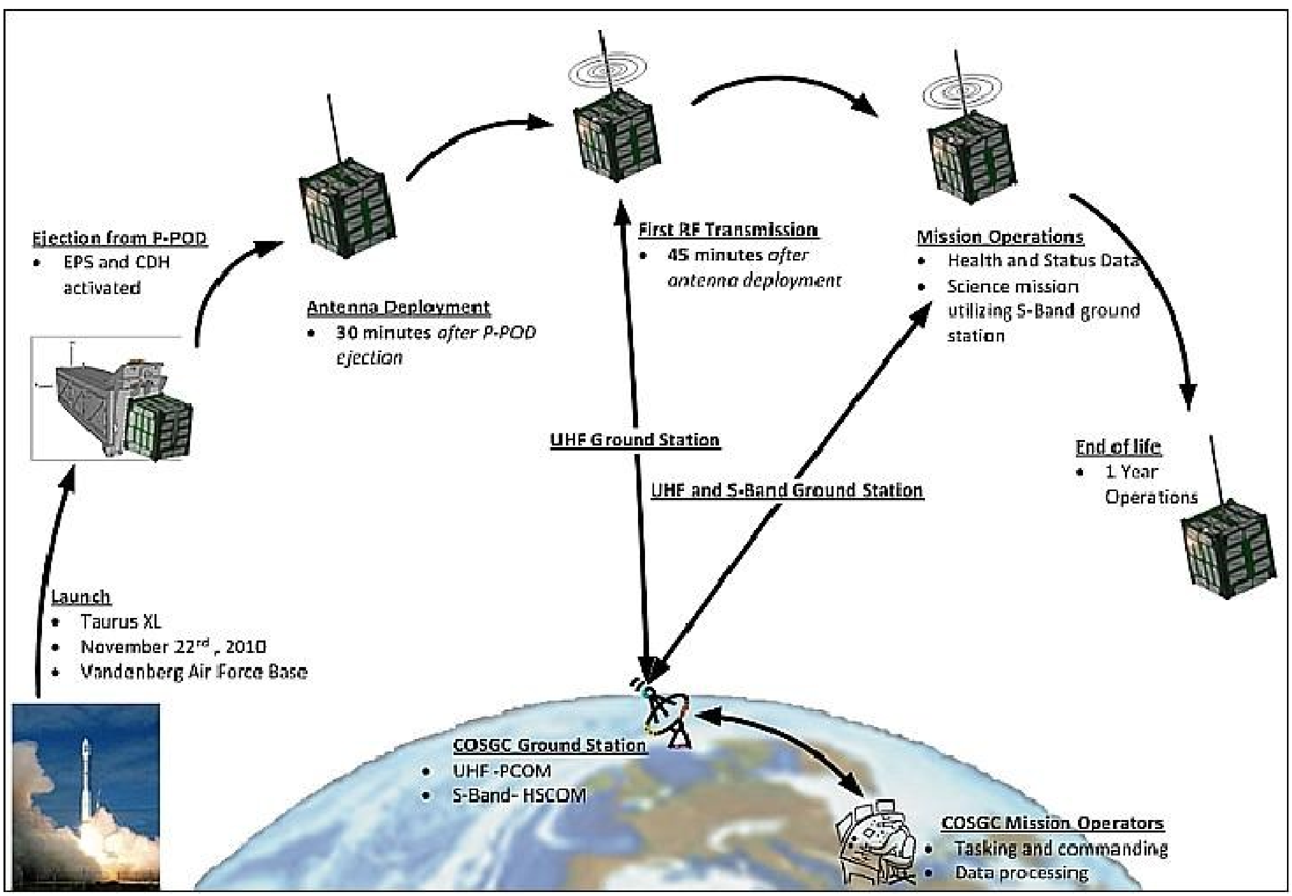

Figure 12: Sketch of the CubeSat launch operations concept (Courtesy: Colorado Space Grant Consortium, USA) [21]

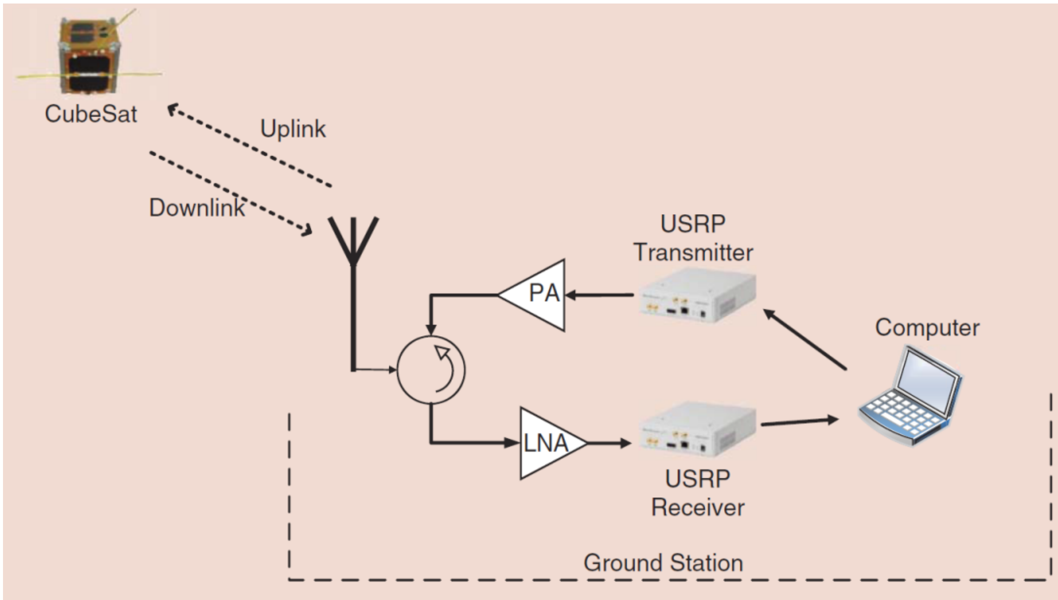

Figure 13: A typical schematic of general CubeSat communication setup [22]

The basic subsystems that make up the internals of a CubeSat are the telemetry, tracking and control (TTC), power generation and distribution (PGD), data command and handling (DCH), altitude determination and control (ADC), and the payload. The commercially available technology is unable to cope with the increasing demand in lower profile and high performance electronic devices for small Satellite applications that can replace the task of large Satellite because of size constraint.

As shown in Figure (13), antenna size plays critical limitation in small satellites. The maximum possible gain of a conventional aperture antenna is determined by the size of the aperture. Hence, dish reflectors, horn antennas, array antennas and other electrically large antennas may have large gain due to their large aperture area. Existing horn antennas have adequate performance, but its large size makes unfriendly for space application. Modifications enabled by smart material can either enhance performance, or they can lower the mass and thus lower the cost of putting the antenna in space. Lighter antennas cost less to boost into space and more energy-efficient antennas can reduce the size of storage batteries and solar cells, which also reduces the mass. Metamaterial lined Horn antennas with low-index electromagnetic properties[24,] shown in Figure (14) is relatively smaller size but yet not suitable for small Satellite (CubeSat) applications[24]. The antenna for small Satellite is an important element for sensors applications. The ongoing research towards developing miniaturized low-index metamaterial lens antenna for small Satellites invites many challenges such as bandwidth and efficiency. Metamaterial lenses exhibit material properties that approximate the behavior of a material with low ($0<n<1$) effective index of refraction, using dispersion techniques a relatively wide-band low-index region can be obtained. A low-index metamaterial lens created highly collimated beams in the far-field from a low directivity antenna feed. For example, dual-split ring resonators (DSRR) in the x-y plane for a low permeability response, and end-loaded dipole (ELD) elements in the x-z and y-z planes for a low permittivity response.

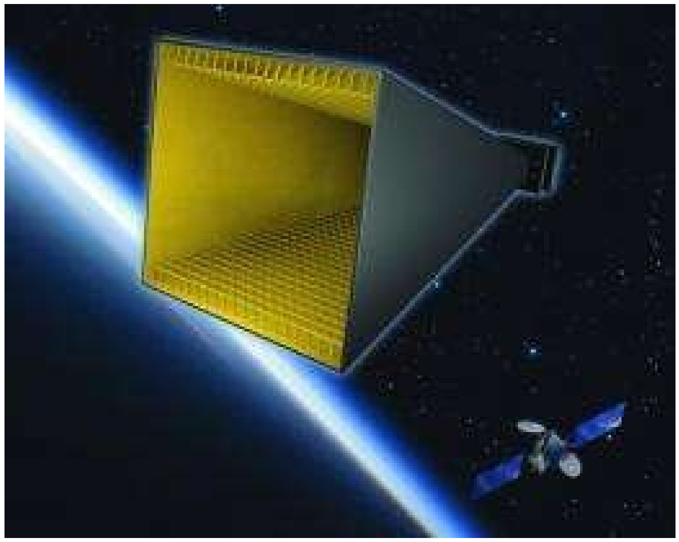

Fig. 14: Shows the typical Metamaterial lined feed horn antenna with low loss, low weight, and over an octave bandwidth for satellite communications shown with satellite [24]

As ε or μ approaches zero, the pass-band narrows, improving collimation and directivity of the antenna, can be integrated with software defined radio (SDR), facilitating a transformative communication system with remarkable frequency and polarization agility; well suited for CubeSat application where multifunctional miniature antennas is desired goal.

The smart material such as MMI (Möbius Metamaterial Inspired) structure technology supports miniaturized multifunctional antenna, high efficiency solar panel for power generation, and can perform the real-time analog signal processing of electromagnetic wave at very high frequencies. Tunable metamaterial using Möbius topology allows broadband tuning in compact size with narrow instantaneous bandwidths across an entire communications band depending on the channel in use. Tuning the metamaterial and antenna in tandem provides a dynamic operating channel, with a tunable, nearly-arbitrary polarization response as an added benefit; enable to devise a way to dynamically tune the frequency response and polarization for the antenna, while, at the same time, providing a pathway to scaling the designs to low frequencies. The major challenge is figuring out a way to scale these metamaterial and associated antenna structures down to operate at lower frequencies while maintaining a practical physical size and weight for the resulting integrated device in general, the lower the frequency, the bigger the antenna. Mobius Metamaterial Inspired antenna allows planar configuration in reduced size at lower frequency without degrading the performance.

(C) Möbius Transformation: Metamaterial Symmetry

The concept of the Möbius Strip is based on fact that one can travel without encountering obstruction around the loop, the loop shall behave like never ending point, gives the conception of infinite journey path in space-time domain. The concept of infinity is not emptiness or space; it has no beginning and no ending. Figure (15a) shows the typical Möbius strip, which gives the notion of no beginning and no ending similar to infinity of emptiness or vacuum. As shown in Figure (15b), the Möbius strip with 1-twist and pinched in the middle appears like the symbol for infinity in mathematics. Since space-time is curved, it could conceivably run back on itself like the Möbius strip, and have no boundary! Our universe can be considered as a replica of the Möbius strip with a multiple number of twists of the vibrating strings in space, whirling in a warped loop as it experiences its own starting point, and recurs perpetually in space-time dynamics. These “strings” vibrate in multiple dimensions, and depending upon how they vibrate, they might be seen in 3-dimensional space as matter, light, or gravity. Figure (15c) shows the 3-twist Möbius Strip, twist can be defined as knots.

(a) Möbius strip (b) Möbius strip pinched in the middle (c) Mobius Strips with 3-twists

Fig.15: A typical Möbius strip: (a) Mobius Strips with 1-twist, (b) Möbius strip with 1-twist and pinched in the middle resembles the symbol for infinity (∞), and (c) 3-twist Möbius Strip with 3-twists.

For engineers, multi-knots Möbius-Strips surface is a launch pad to complex geometries and topological exploration for next generation electronic circuits and systems for industrial, medical, and space applications. Topology is a field of science that studies invariance of certain properties under continuous deformation, such as stretching, bending, or twisting, of the underlying geometry. Topological symmetry defined as a property, conserved when the system undergoes an alteration (deformation, twisting and stretching of objects), for example, Möbius strips deform in a way that its metrical properties barely change, and violate the Hückel rules[25]; for example, some nanostructures posses the identical elastic properties even after deformation. It is interesting to note that the Möbius transformations allow complex geometries for realization of number of distinct types of Metamaterials. Metamaterial structure can be realized by either array of wire/split-ring structure or composite right/left-handed (CRLH) transmission line resonators. The major difference between two metamaterial structures is the coupling dynamics; wire/split-ring structure is loosely coupled, whereas CRLH transmission line resonators structure is tightly coupled. Since wire/split-rings structures is practically uncoupled, therefore operating bandwidth is determined by their quality factor and loss associated with wire/split-ring structures. The real challenge faced by designer to reduce the losses and improve the quality factor of these structures. In the case of CRLH transmission line resonators based metamaterial structures, the resonators are coupled, and therefore increase the operating bandwidth as compared to wire/split-rings based metamaterial structure[7]

The topological Möbius metamaterial symmetry is due to Möbius transformation characteristics $f(z)$, is given by[26]

$$f(z) = \frac{az+b}{cz+d}\,;\ \ (\text{a, b, c, d} \in \mathbb{C} \text{ and } ad - bc \neq 0) \tag{1}$$

$$\text{z} \in \mathbb{C} \rightarrow z = r[cos(\theta) + isin(\theta)] \tag{2}$$

where a, b, c, and d are complex numbers, and the numerator of (1) is not a multiple of denominator (i.e. $ad - bc \neq 0$).

From (2), the properties of Möbius transformation $f(z)$ are

(i) $f(z)$ *can be expressed as a composition of affine transformations (scaling:* $z \rightarrow tz$*, translation:* $z \rightarrow z + p$*, rotation:* $z \rightarrow e^{i\theta} z$ *, complex conjugation:* $z \rightarrow \bar{z}$*, inversion:* $z \rightarrow \frac{1}{z}$ *), where t, p* $\in \mathbb{C}$

(ii) $f(z)$ *maps* $\mathbb{C}$ *one-to-one onto itself, and is continuous*

(iii) $f(z)$ *maps circles and lines to circles and lines*

(iv) $f(z)$ *is conformal*

From (i)-(iv), the family of functions is the composition of functions; the identity element is the identity map, and the inverse is given by inverse function. The Möbius group consists of those fractional linear transformations, which maps the open unit disk $\mathbb{D} = \{z \in \mathbb{C}: |z| < 1\}$ to itself in a one-to-one way. These transformations and their inverses are analytic on $\mathbb{D}$ and map its boundary (the unit circle S^1=$\{z \in \mathbb{C}: |z| < 1\}$ to itself. The automorphisms of the disk is in the form:

$$f(z) = e^{j\varphi} \frac{\alpha - z}{1 - \bar{\alpha} z} \quad (3)$$

$$z = M(w) = \frac{e^{j\psi} w + \alpha}{1 + \bar{\alpha} e^{\psi} w} \quad (4)$$

$$w = M^{-1}(z) = e^{-j\psi} \frac{z - \alpha}{1 - \bar{\alpha} z} + a \quad (5)$$

where $\varphi \in \mathbb{R}$, $\psi \in \mathbb{R}$, and $\alpha \in \mathbb{D}$.

From (1)-(5), Möbius transformation can be used for Möbius Metamaterial symmetry, which has received widespread attention in the field of metamolecules, optical polarization, DNA (Deoxyribonucleic acid) sensor, and high frequency components for energy saving electronics and instrumentation[26-35] .

Examples: Möbius Metamaterial Symmetry

(i) Benzene Metamolecules

The electromagnetic (EM) symmetry discovered in the metamaterial is equivalent to the structural symmetry of a Möbius-Strip, with the number of twists controlled by the sign change of the electromagnetic coupling between the meta-atoms. Figure (16) illustrates the Metamaterial Möbius symmetry made from metals and dielectrics[27]. As depicted in Figure (16), the hyperspace Möbius mechanism transforms ordinary benzene molecules into metamolecules with Mobius symmetry: "the topological phenomenon that yields a half-twisted strip with two surfaces but only one side". The prototype of metamolecular trimer shown in Figure (16) is a 3-body system like a trimmer, metallic resonant meta-atoms configured as coupled split-ring resonators, symbolized as metamolecules exhibits topological Möbius-Cyclic-Symmetry (C_3-symmetry) through 3- rotations of 120-degrees, and Möbius-twists result from a change in the signs of the electromagnetic coupling constants between the constituent meta-atoms[27]. The interesting phenomena is "with different coupling signs exhibit resonance frequencies that depend only on the number of turns but not the locations of the twists,'' thus confirming its Möbius Symmetry.

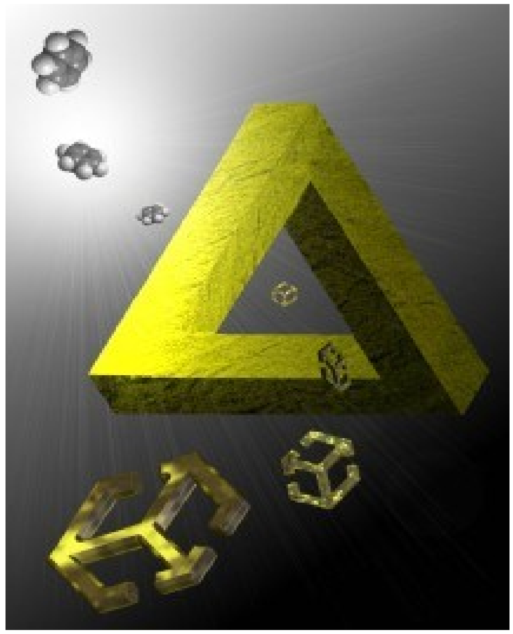

(b) Metamolecular trimer

Fig. 16: Möbius-Strips symmetry in metamolecular trimers [27]

(ii) Polarized Light

Figure (17) illustrates the artificial Möbius Strip formed by EM (electromagnetic wave) waves, which demonstrates “a light-beam can be controlled so that its polarization twists follow a contour of Möbius-Strips”[28]. The creation of EM (electromagnetic) wave around Möbius contour is interesting for improving the fundamental understanding of optical polarization and the complex light beam engineering for developing optical micro-and nano-fabrication structures for sub-wavelength imaging. As shown in Figure (17), the typical Möbius strip surface made of polarized states of light beam, which is a non-vanishing curvature, and exhibits spatial symmetry.

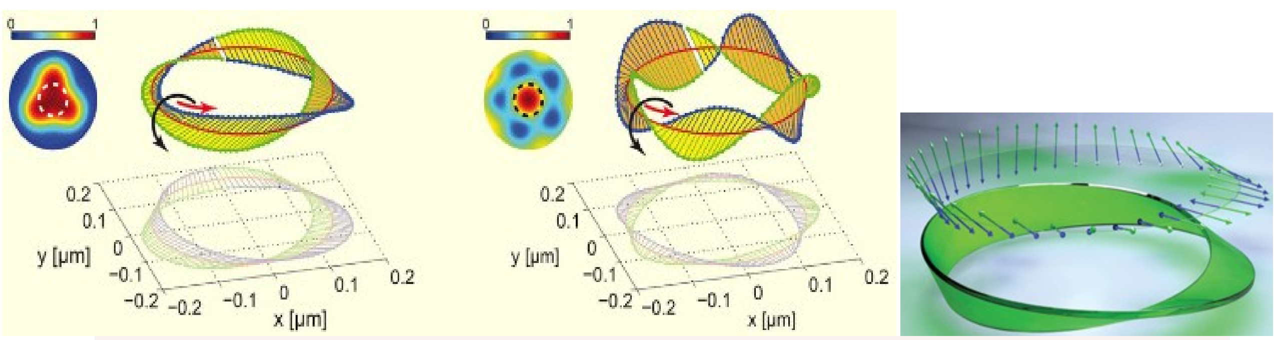

(a) single knot (b) multi-knots (c) polarization twist

Fig. 17 shows the numerically calculated and experimentally observed optical polarization twist around the Möbius strips [28]

***(iii)* DNA Strip Sensor**

Figure (18) shows the nano-architectures of Möbius DNA (Deoxyribonucleic acid) strip in which each colored band represents a different DNA double helix; such nano-architectures can be used in high sensitivity biological and chemical sensing devices [29].

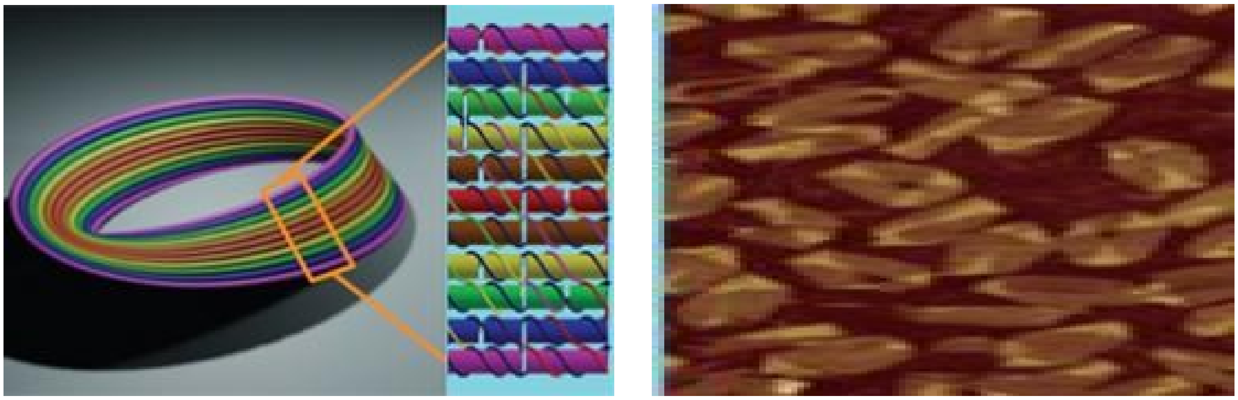

Fig.18: The typical nano-architectures of Möbius DNA strip: (a) colored Möbius strip, (b) A fraction of the Möbius strip in (a) is illustrated in the DNA helical mode, and (c) Image of Möbius DNA strip [29].

***(iv)* MMI (Möbius Metamaterial Inspired) Graphene**

Recently, Graphene has received extensive attention due to its remarkable structural (single layer of graphite, exhibits mechanical properties like thin paper or plastic with large bulk modulus along the plane of Graphene, easily bent or curved) and superior electronic and optical properties[30]. This unique characteristic allows Graphene to wrap into carbon nanotubes without deformation, qualifies to use Graphene to build Möbius-Strips for microwave and optical components for next generation communication systems. The bandgap and cohesive energy of Mobius Graphene as depicted in Figure (19) depends on the width of strip, and augmented by increasing the width, described by [31]

$$E_{C0}^{r(M)} = \frac{E_{SCF}^{r(M)} - N_C \times E_{SCF}^{C} - N_H \times E_{SCF}^{H}}{\sum(N_C + N_H)} \tag{6}$$

where the superscript *r(M)* corresponds to the Graphene ribbon (Mobius strip), N_C is the number of carbon atoms, N_H is the number of hydrogen atoms, $E_{C0}^{r(M)}$ is the self-consistent field energy of the Graphene ribbon (Mobius strip), E_{SCF}^{C} and E_{SCF}^{H} are the self-consistent field energy of alone carbon and hydrogen atoms, respectively.

The magnetic moment and spin-properties of Möbius Graphene is very interesting. It is interesting to note that Graphene Möbius strip keeps its metallic surface states in the presence of an external electric field. For sufficiently higher applied electric field, the spin flipping can take place in the Mobius strip. In contrast with the Graphene nanoribbons, Graphene Mobius strips show half-semiconducting properties when an external electric field is applied.

Figure (20) shows the typical orbital of Graphene Möbius strip and spin dependent DOS (density of states). As shown in Figure (20), ferromagnetism and spin-flipping properties of Möbius Graphene makes attractive applications for spintronic devices and quantum oscillator applications[31].

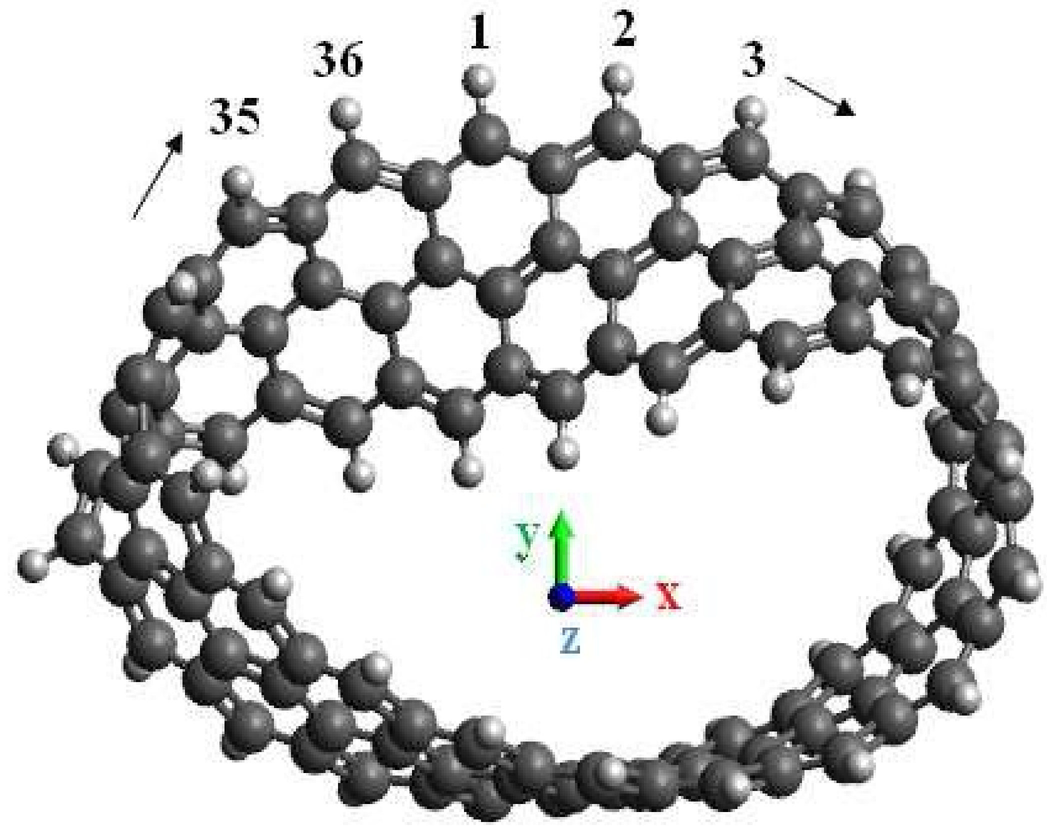

Fig.19: Graphene Möbius structure: Mobius strips with length L=18 and width N=3 (Möbius axis and edge C atom index are shown) [31]

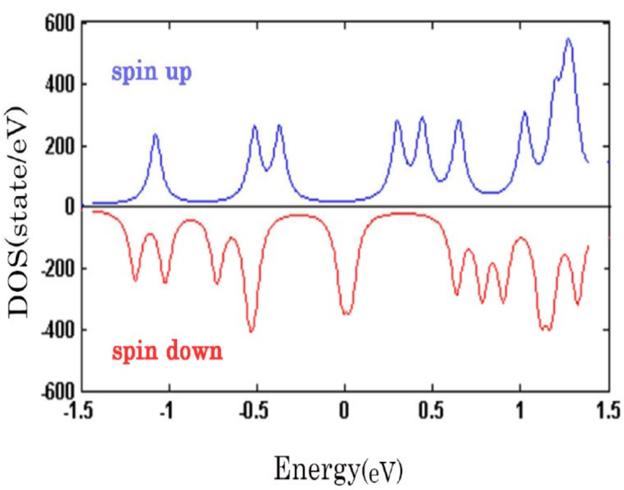

(a) Spin dependent DOS

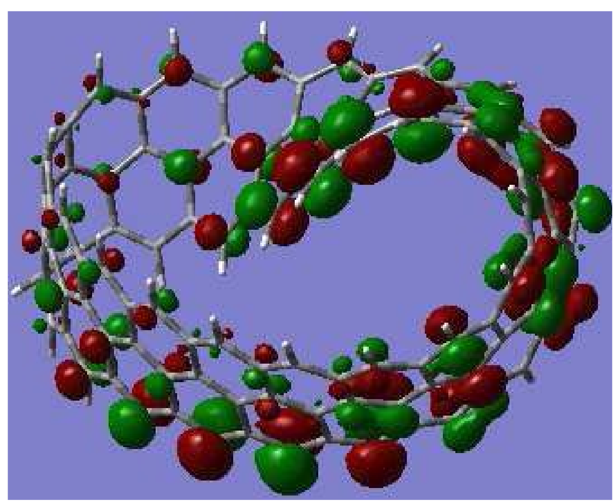

(b) Orbital of Graphene Mobius Strip

Fig.20: (a) depicts spin-dependent DOS (density of states) of Graphene Möbius strip as a function of the electron energy, and (b) molecular orbital of Graphene Möbius strip at E=0eV [31]

Figure (21) shows the characteristics of Möbius molecular rings that support metamaterial characteristics (negative permittivity ε and negative permeability)[32].

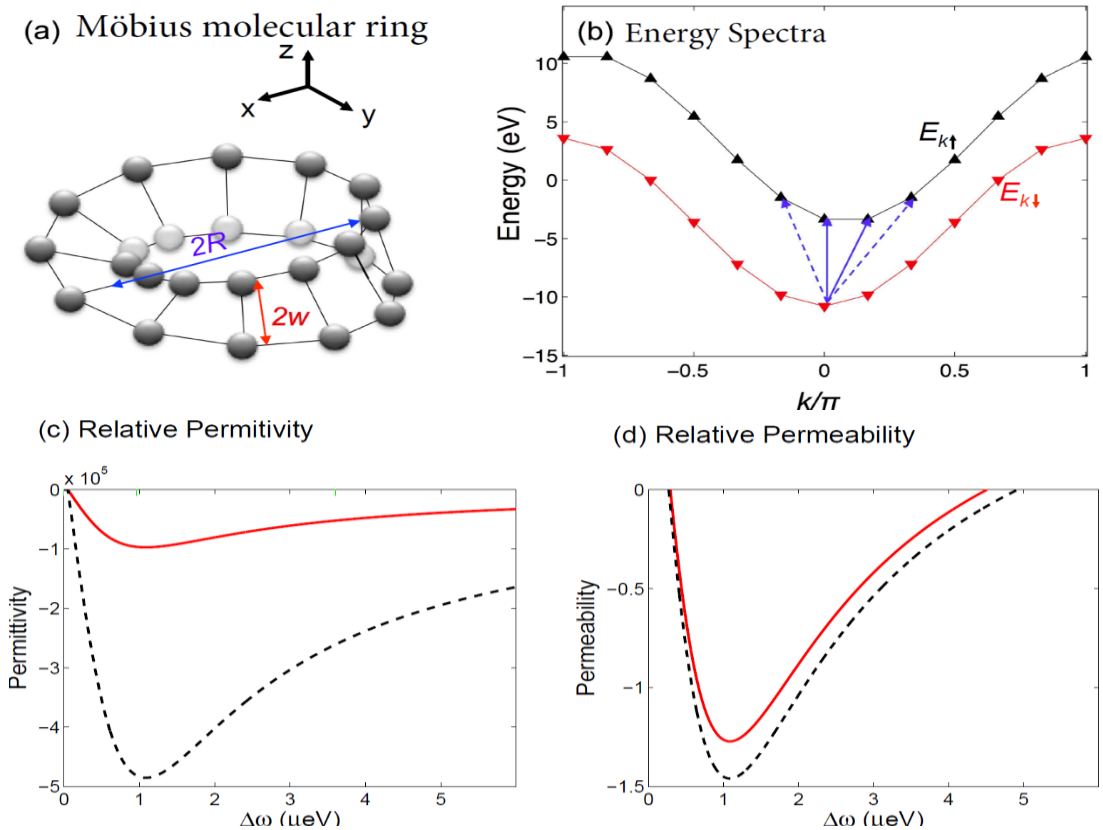

Fig. 21: (a) Möbius molecular rings made of carbon atoms, (b) Energy spectra $E_{k\sigma}$ of the molecular ring, (c) Relative permittivity as a function of Δω, and (d) Relative permeability as a function of Δω [32]

As shown in Figure (21), two energy bands are denoted by their different pseudo spin labels σ =↑and↓; detuning $\Delta\omega = \omega - \Delta_0$[32].

The difference between the Möbius molecular ring and the common annulenes lies in the boundary condition. The negative index properties offer remarkable properties such as image cloaking, sub-wavelength imaging, enhancement of evanescent fields resulting improved Q-factor.

Figure (22) depicts the application of Graphene Möbius strips for the realization of microelectronic components[30-35].

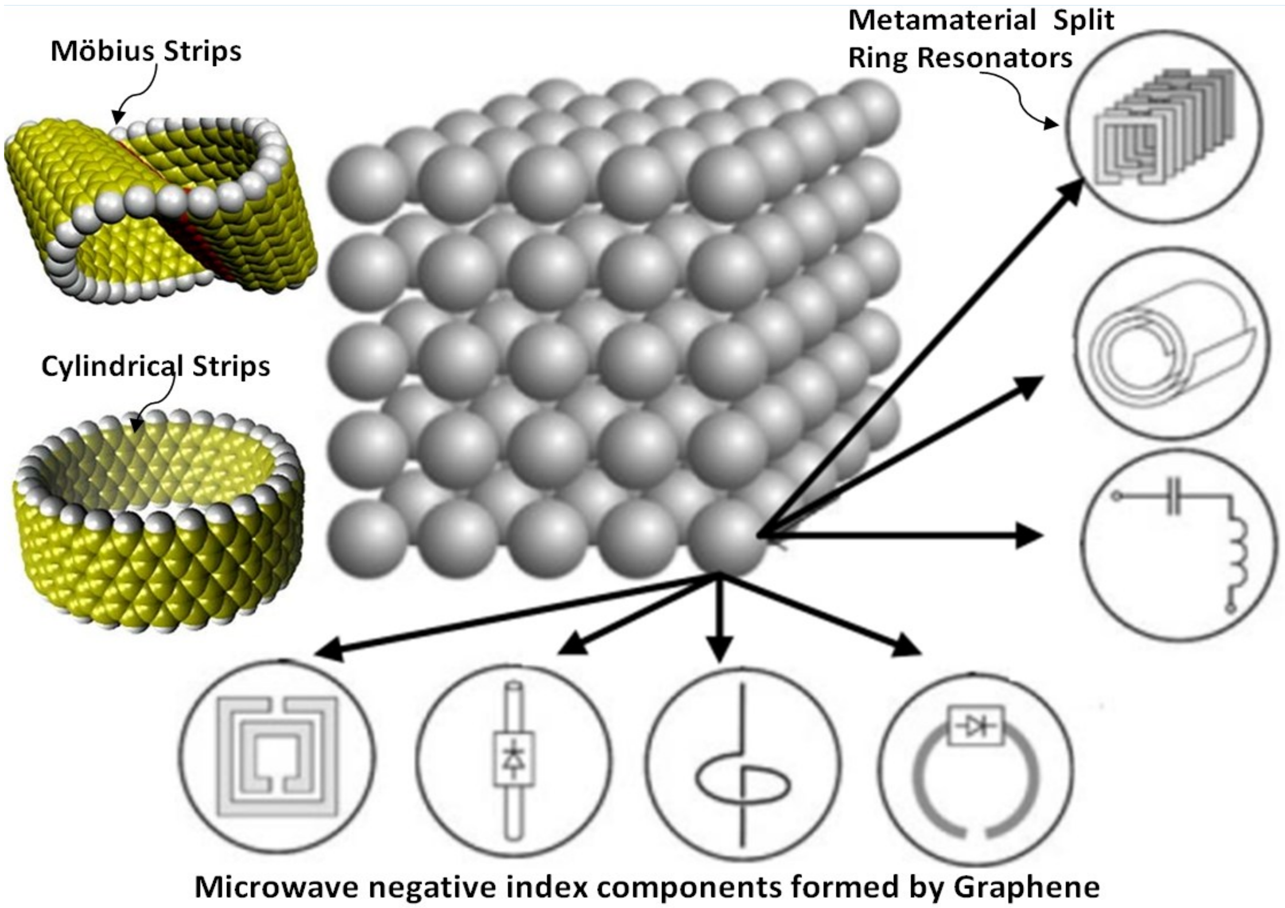

Fig.22: The structures of the Möbius Metamaterial strips formed by Graphene for the realization of microelectronic components [30]

Figure (22) illustrates the next generation microwave components realized by Möbius Metamaterial strips, the electromagnetic coupling dynamics govern by Möbius transformation.

As shown in Figure (22), cylindrical closed ring strips structures formed by Graphene-nanoribbons possess 2-edges, exhibit anti-ferromagnetic (Zero-magnetic moment, whereas Mobius closed ring strips structure formed by Graphene-nanoribbons possess single-edge, exhibit ferromagnetism (nonzero magnetic moment). Graphene nanoribbons with 'zigzag' edge structure exhibits magnetism at their edges, most stable configuration of these ribbons is anti-ferromagnetic, so that magnetic moments at opposite edges point in opposite directions, reducing the total magnetic moment of the ribbons to zero. However, Graphene Möbius strip is only one continuous edge, hence no magnetic cancellation between the opposite edges, resulting nonzero magnetic moment.

(v) Medical Telemetry

Medical telemetry systems in medicine have considerably increased due to inevitability for early diagnosis of diseases and continuous monitoring of physiological parameters. Microwave antennas and sensors are key components of these telemetry systems since they provide the communication between the patient and base station. The Industrial, Scientific and Medical (ISM) radio bands are portions of the radio spectrum reserved internationally for the use of radio frequency (RF) energy for industrial, scientific and medical purposes other than communications. By using metamaterial like

EBG (Electromagnetic Band Gap) structures in slotted microstrip antenna the increased efficiency and better return loss characteristics can be achieved [36].

Cancer is the uncontrolled growth of abnormal cells in the body, called as malignant cells. By developing microwave devices and combining it with structures inspired by Metamaterials, it can lead to a very cost-effective device that can localize with high precision an abnormality within the human body. The basic principle behind the cancer detection is, a small change in the water content of biological tissues produces changes in the permittivity (ε) and conductivity (σ) values of the tissues[37]. The malignant cells have significantly higher water content than normal tissues. Hence the permittivity and the conductivity of the tumor are higher than those ones of a normal tissue at microwave frequencies. The proposed biosensor consists of an array of complementary metallic metamaterial resonators. The reasons for choosing SRRs (Split ring resonators) are their strong response to an electromagnetic field[37]. An electromagnetic source generates an electromagnetic wave impinging on the metamaterial array and a detector is placed to reveal the signal after the array. The biosensor without any material under test has a specific resonant frequency[37]. The variation of the permittivity caused by the presence of the material under test, acts on the capacitance of the resonators, leading to a high sensitive variation of the sensor resonant frequency. Thus the shift in resonant frequency and the shape of the response is extremely useful to detect the tumor. Figure (23a) shows the typical metamaterial inspired coupled SRR based sensor comprised of 12 SRRs, represents a pixel of the relative dielectric behavior of the material under test (MUT).

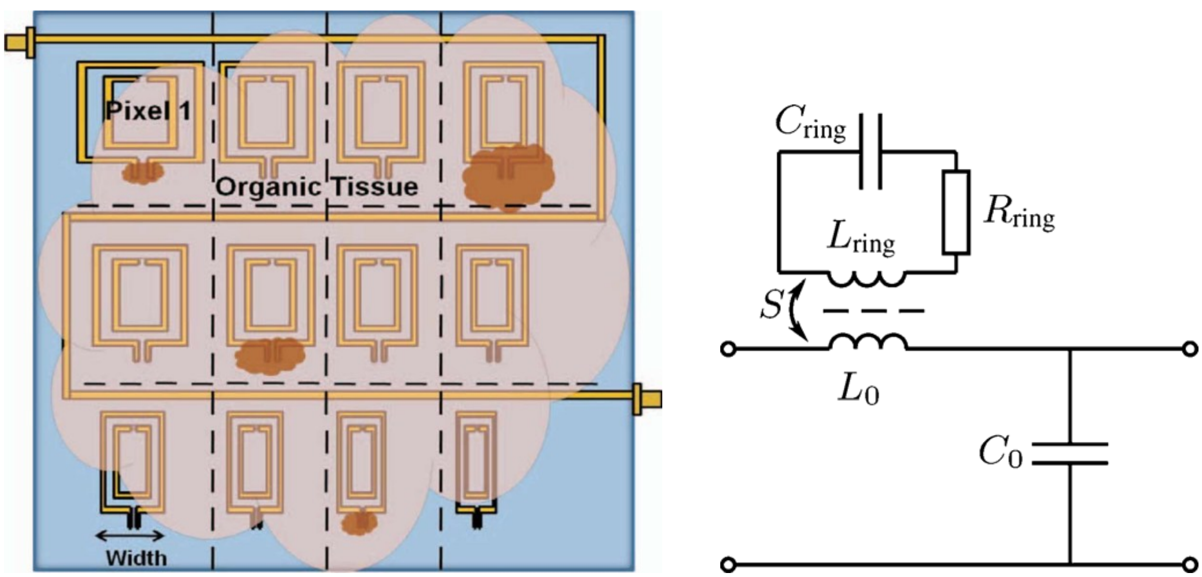

(a) Metamaterial inspire microstripline coupled SSR sensors microstripline

(b) Equivalent lumped module of a SRR loaded

Figure 23: Schematic of the multiplexed 2-D sensor array made of 12 pixels. The sensitivity region of the sensor corresponds to the complete surface of the structure where a sample of the organic tissue is shown with some pieces of malignant tissues around the first, fourth seventh and eleventh pixel [27]-[28].

For example, if a perturber, such as an organic tissue, interacts with the outer split of a SRR it changes the capacitance value due to a change of the effective permittivity and therefore differences on the tissues, such as abnormalities, can be detected [38]. The equivalent circuit of a microstrip line loaded with a single SRR[39] for the quasi-static case is shown in Figure (23b). The SRR is magnetically coupled to the transmission line with the coupling factor and corresponds to the total

SRR inductance and capacitance, respectively. The equivalent circuit yields the effective permeability with Lorentz dispersion[40]

$$\mu_{eff}=-j\frac{Z_1}{\omega p}=\frac{L_0}{p}\left(1+\frac{\omega^2 S^2}{\omega_{0m}^2-\omega^2+j\omega\delta}\right) \tag{7}$$

with p being the net cell length.

(vi) Acoustic imaging

Acoustic imaging tools are used in both medical diagnostics and in testing the structural integrity of everything from airplanes to bridges. Medical personnel and structural engineers often need to focus sound for imaging or therapeutic purposes. Metamaterial gives researchers more control over the angle at which acoustic waves can pass through it. Figure (24) shows the typical metamaterial inspired acoustic hyperbolic structure made of paper and aluminum for acoustic imaging application. As shown in Figure (24), the AHM (acoustic hyperbolic metamaterial) structure allows it to manipulate acoustic waves to more than double the resolution of acoustic imaging, focus acoustic waves, and control the angles at which sound passes through the metamaterial[41].This means that it interacts with acoustic waves in two different ways. From one direction, the metamaterial exhibits a positive density and interacts with acoustic waves normally- just like air. But from a perpendicular direction, the metamaterial exhibits a negative density in terms of how it interacts with sound. This effectively makes acoustic waves bend at angles that are the exact opposite of what basic physics predicts. The practical effect of this is that the metamaterial has some very useful applications. For one thing, the metamaterial can be used to improve acoustic imaging. Traditionally, acoustic imaging could not achieve image resolution that was smaller than half of a sound's wavelength. For example, an acoustic wave of 100 kilohertz (kHz), traveling through air, has a wavelength of 3.4 millimeters (mm) - so it couldn't achieve image resolution smaller than 1.7 mm.

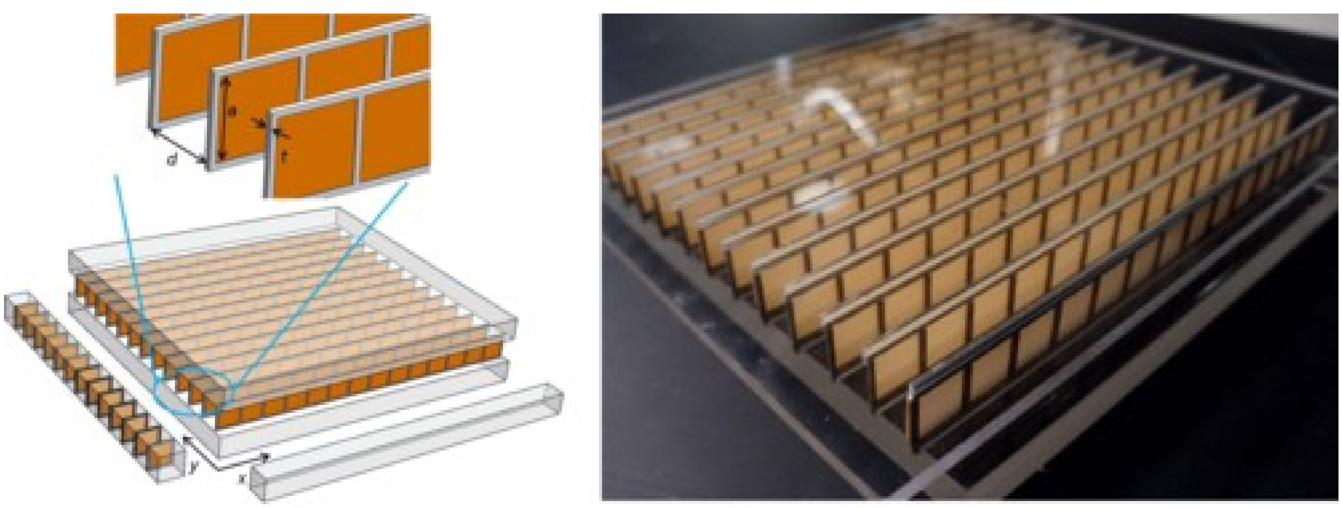

Figure 24: shows the typical Physical structure of the AHM (acoustic hyperbolic metamaterial): metamaterial inspired AHM structure made of paper and aluminum for acoustic imaging.

Conclusion:

The unique features of MMI (Möbius Metamaterial Inspired) structure open the gateway to new inventions in the future, recurring in an endless fashion–one could even say that everything is going to be in the future in the form of MMI Surface. In this article, Casimir Effect is discussed briefly, details of Casimir Effect and applications using MMI (Möbius Metamaterial Inspired) structure for futuristic applications will be discussed in Part-2 (June 2016 Issue) and Part-3 (July 2016 Issue).

Reference

[1] U. L. Rohde, A. K. Poddar, "Möbius Strips and Metamaterial Symmetry: Theory and Applications", Microwave journal, Nov 2014, pp. 76-88.

[2] U. L. Rohde, A. K. Poddar, "Möbius Metamaterial Strips Resonator for Tunable Oscillators for Modern Communication Systems", Part-3, Microwave journal, Jan 2015

[3] U. L. Rohde, A. K. Poddar, "Möbius Metamaterial Strips Resonator for Tunable Oscillators for Modern Communication Systems", Part-3, Microwave journal, Jan 2015

[4] A. Poddar, "Slow wave resonator based tunable multi-band multi-mode injection-locked oscillator", Habil Thesis, BTU Cottbus, Germany, 2014

[5] U. L. Rohde, A. K. Poddar, D. Sundarrajan", Real Time Signal Retention Device using Co-planar Waveguide (CPW) as Mobius strip", 2013 IEEE MTT-S Digest, pp. 1-3, June 2013

[6] U. L. Rohde, A. K. Poddar, D. Sundarrajan", A Novel Mobius-Coupled Printed Resonator Based Signal Sources", 2013 IEEE MTT-S Digest, pp. 1-3, June 2013

[7] C. Caloz, "Perspectives on EM Metamaterials," *Materials Today*, vol. 12, no. 3, pp. 12–20, Mar. 2009, *invited*.

[8] C. Caloz, "Tomorrow's Metamaterials: Manipulation of Electromagnetic Waves in Space, Time and Space time", http://arxiv.org/pdf/1602.04340.pdf

[9] Astrid Lambrecht, "The Casimir effect: a force from nothing", Physics World, Sept 2002, IOP Publishing Ltd 2014, ISSN: 0953-8585

[10] Ran Zeng, Yanjun Chen, and Yaping Yang, "Stable multilayer structure based on restoring Casimir forces", Eur. Phys. J. B (2013) 86: 398, DOI: 10.1140/epjb/e2013-40748-0

[11] http://cnls.lanl.gov/casimir/PostersSF/Intravaia-SantaFe-poster.pdf

[12] Ulf Leonhardt and Thomas G. Philbin, "Quantum levitation by left-handed Metamaterials", arXiv:quant-ph/0608115

[13] James Q. Quach, "Gravitational Casimir effect", Phys. Rev. Lett. 114, 081104 (2015), 0.1103/PhysRevLett.114.081104

[14] https://en.wikipedia.org/wiki/Internet_of_Things

[15] C. Caloz, "Metamaterial dispersion engineering concepts and applications,"*Proc. IEEE*, vol. 99, no. 10, pp. 1711–1719, Oct. 2011

[16] B. E. A. Saleh and M. C. Teich, *Fundamentals of Photonics*, 2nd ed, wiley, 1964, Chap. 22.

[17] C. Caloz, S. Gupta, Q. Zhang, and B. Nikfal, "Analog signal processing, "*IEEE Microw. Mag.*, vol. 14, no. 6, pp. 87–103, Sept. 2013, *invited*

[18] https://en.wikipedia.org/wiki/ESTCube-1

[19] https://directory.eoportal.org/web/eoportal/satellite-missions/h/hermes

[20] http://www.nasa.gov/mission_pages/cubesats/index.html

[21] NASA CubeSat launch, http://southgatearc.org/news/january2010/nasa_cubesat_launch.htm

[22] Garrett L. Skrobot, "Project ElaNa and NASA's CubeSat Initiative," Proceedings of the Cal Poly 2010 CubeSat Developer's Workshop, San Luis Obispo, CA, USA, April 21-23, 2010

[23] O. Ceylan, A. Caglar, H. B. Tugrel, H. O. Cakar, A. O. Kislal, K. Kula, and H. B. Yagci, " Small Satellites Rock", IEEE Microwave Magazine, pp. 26-33, March 2016

[24] http://phys.org/news/2011-01-metamaterials-approach-satellite-antennas.html

[25] Hückel, E., "Grundzüge der Theorie ungesättiger und aromatischer Verbindunge*n*", Berlin: Verlag Chem, pp. 77–85, 1938

[26] Marvel et al, "Identical phase oscillators with global sinusoidal coupling evolve by Möbius group action", 2009 American Inst. of Physics, pp.1-11

[27] Chang et al, "Optical Mobius Symmetry in Metamaterials", Physical Review Letters, pp. 235501-1-235501-4, Dec 2010

[28] T. Bauer et. al. “Observation of optical polarization Möbius strips”, **Science** DOI: 10.1126/science.1260635, Jan 29, 2015

[29] Han et al, “Folding and cutting DNA into reconfigurable topological nanostructures”, Nature Nanotechnology vol.5, pp 712-717, 2010

[30] Wang et al, “Theortical investifgation of Mobous strips formed from Graphene“, Applied Physics Letters 2010

[31] Mazidabadi et al., “Electronic and Magnetic Properties of Graphene Mobius Strips: Density Functional Theory Approach”, *IJMSA,* Vol. 3, No. 5, 2014, pp. 268-273.

[32] Fang et al, “Negative Refraction Induced by Möbius Topology”, http://arxiv.org/pdf/1501.05729.pdf, Jan 2015

[33] A. Poddar, “Slow wave resonator based tunable multi-band multi-mode injection-locked oscillator”, Habil Thesis, BTU Cottbus, Germany, 2014

[34] Li Guansheng, E. Afshari, “A low phase noise multi-phase oscillator based on left-handed LC-Ring”, JSSC. vol. 45, pp. 1822-1833, Sept 2010.

[35] Rofougaran et al, “A 900 MHz CMOS *LC* oscillator with quadrature outputs,” in *IEEE ISSCC Dig.Tech. Papers*, Feb. 1996, pp. 392–393

[36] Kumar, H., R. K. Kanth, P. Liljeberg, and H. Tenhunen, \Metamaterial based slotted patch antenna," *IEEE 10th International Conference on Telecommunication in Modern Satellite Cable and Broadcasting Services (TELSIKS)*, 43{46, 2011.

[37] La Spada, L., F. Bilotti, and L. Vegni, \Metamaterial biosensor for cancer detection," *IEEE Sensors*, 627{630, 2011.

[38] Puentes, M., M. Maasch, M. Schubler, and R. Jakoby, \Frequency multiplexed 2-dimensional sensor array based on split-ring resonators for organic tissue analysis," *IEEE Trans. on Microwave Theory and Tech.*, Vol. 60, No. 6, 1720{1727, Jun. 2012.

[39] J. Baena, J. Bonache, F. Martin, R. Sillero, F. Falcone, T. Lopetegi, M. Laso, J. Garcia-Garcia, I. Gil,M. Portillo, and M. Sorolla, “Equivalent circuit models for split-ring resonators and complementary split-ring resonators coupled to planar transmission lines,” *IEEE Trans. Microw. Theory Tech.*, vol. 53, no. 4, pp. 1451–1461, Apr. 2005.

[40] A. Trehan and N. Nikolova, “Summary of materials and recipes available in the literature to fabricate biological phantoms for RF and microwave experiments,” Ph.D. dissertation, Computational Electromagnetics Lab., Dept. Elect. Comp. Eng., McMaster University, ON, Canada, 2009

[41] Chen Shen, Yangbo Xie, Ni Sui, Wenqi Wang, Steven A. Cummer, and Yun Jing, “Broadband Acoustic Hyperbolic Metamaterial”, Phys. Rev. Lett. 115, December 2015